

# **EXPERIMENTAL CALIBRATION OF A NUMERICAL MODEL OF PREPREG TACK FOR PREDICTING AFP PROCESS RELATED DEFECTS**

Alireza Forghani<sup>1</sup>, Curtis Hickmott<sup>1</sup>, Victoria Hutten<sup>1</sup>, Houman Bedayat<sup>1</sup>, Christopher Wohl<sup>2</sup>, Brian Grimsley<sup>2</sup>, Brian Coxon<sup>1</sup>, Anoush Poursartip<sup>1,3</sup>

<sup>1</sup> Convergent Manufacturing Technologies US, Seattle, WA

<sup>2</sup> NASA Langley Research Center, Hampton, VA

<sup>3</sup> Department of Materials Engineering, The University of British Columbia, Vancouver, BC, Canada

## **ABSTRACT**

Wrinkles, puckers, and fiber bridging are among the major defects encountered in the Automated Fiber Placement (AFP) process, and are all different manifestations of fiber misalignment. The main driver for these defects are the residual stresses introduced in the tow during the deposition stage by the AFP head. In contrast, the tack between the deposited tape and the substrate is the resisting force against the formation of such defects. Tack may be defined as the ability of a material to form a bond immediately on contact with another surface. Tack is a very complex phenomenon that is influenced by a variety of process parameters including temperature, head pressure and speed, as well as degree of cure, moisture content, and surface roughness. A physics-based modeling framework for simulation of tack was developed in this study that allows for prediction of tack response. The developed tack model is incorporated in the AFP placement modelling framework developed to simulate AFP defects.

## **1. INTRODUCTION**

Deposition of prepreg tape during AFP is a very complex process that includes interactions between the AFP head, prepreg tow and the substrate. In the physics-based modeling approach adopted by Convergent Manufacturing Technologies US, the aim is to simulate the major physical phenomena that contribute to the deposition process and consequently lead to formation of AFP defects. Figure 1 shows the preliminary AFP head model that includes a simplified representation of the head, deposited tow and the substrate.

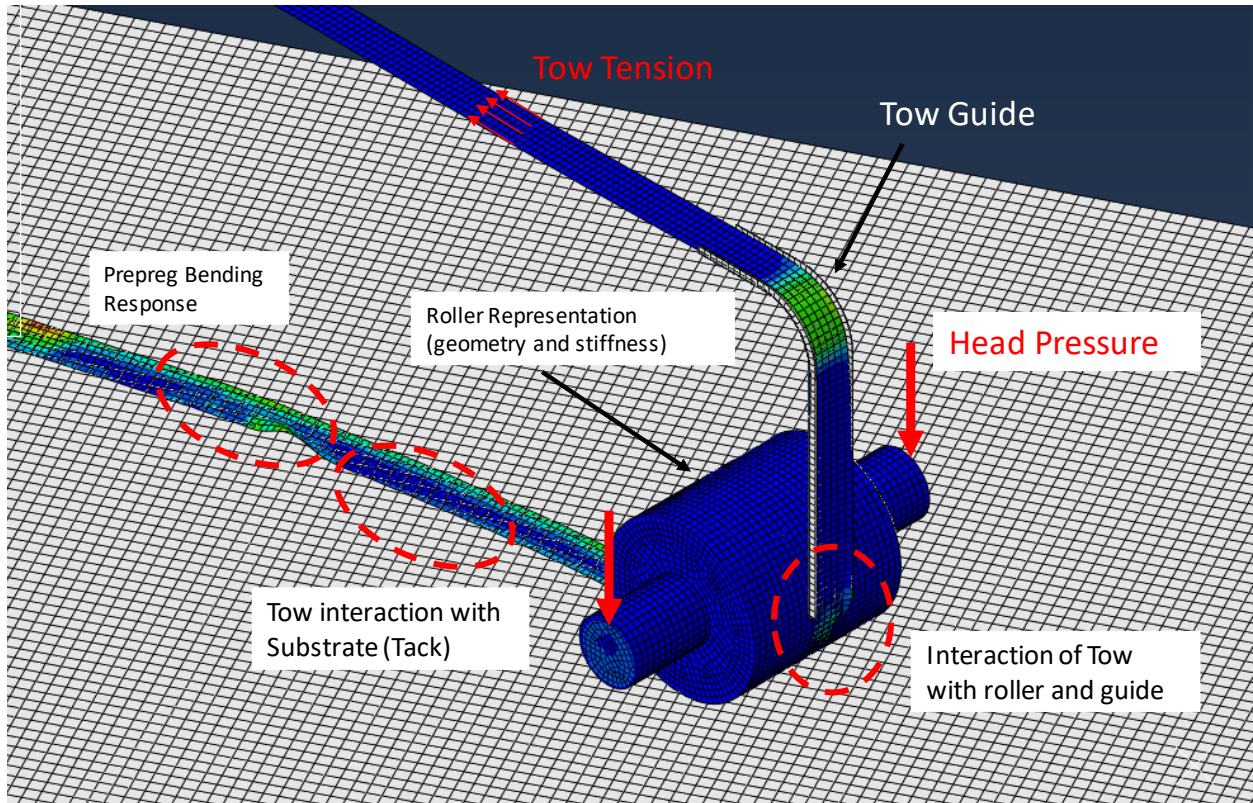


Figure 1 Schematic of the physics-based AFP deposition simulation highlighting the important phenomena captured by the model.

The physical phenomena that contribute to formation of out-of-plane misalignments (e.g. puckers and wrinkles) can be categorized under sources and sinks. Sources are the phenomena that promote the formation of these defects. The main sources include the excess length formed in the prepreg tape as a result of head steering and residual stresses induced during placement. Sinks on the other hand are the phenomena which resist formation of the defects. The adhesion between the prepreg tape and substrate, known as “tack,” is the key resisting phenomenon and accurate modeling of tack is very important in prediction of AFP-related defects.

Experimental observations show that the complex physics of tack depends on many parameters [1-3]. Tack formation during cohesion strongly depends on the history of pressure and temperature experienced by the prepreg during deposition and compaction, while separation of surfaces is dependent on both temperature and peeling rate [2].

In this study, tack phenomena are investigated in two stages, namely cohesion and decohesion. The first stage is the formation of tack (cohesion) where contact between two prepreg surfaces and application of pressure and temperature leads to inter-diffusion, mixing and interlocking of resin between the substrate and the deposited slit tape (called Intimate Contact). The second stage is decohesion where the two faces are forced to separate. The simulation framework proposed here considers both stages (see Figure 2). Figure 3 is a schematic of the dependencies. The Degree of Intimate Contact (DoIC) is a state variable introduced to represent the quality of the cohesion achieved and varies between 0 and 1.

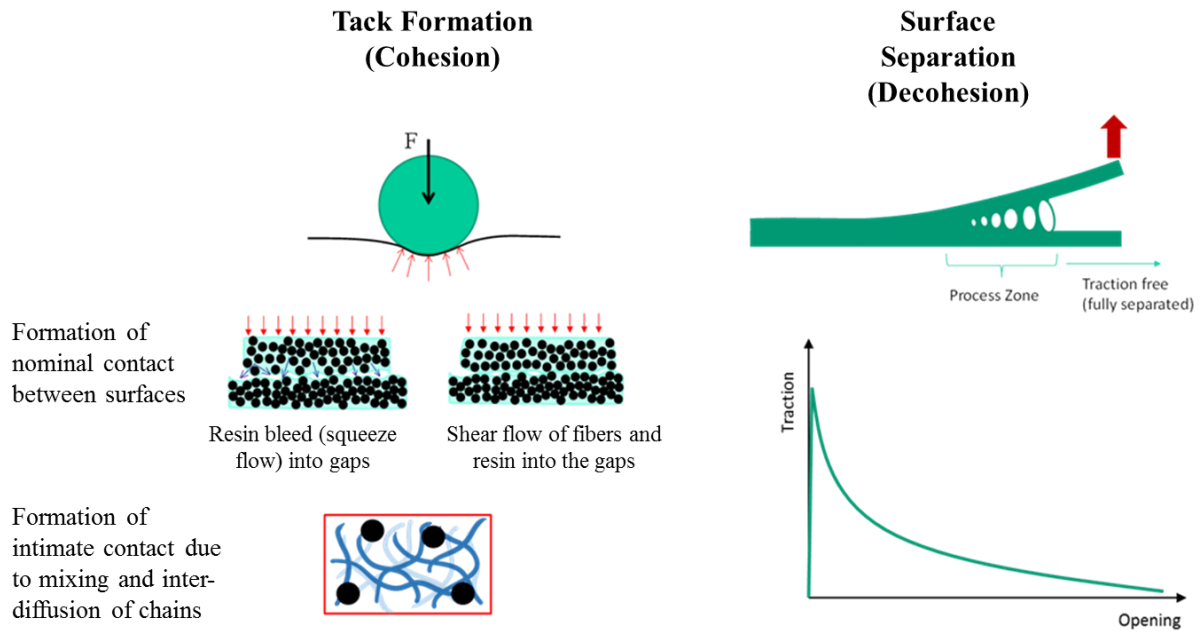


Figure 2 Cohesion and Decohesion stages.

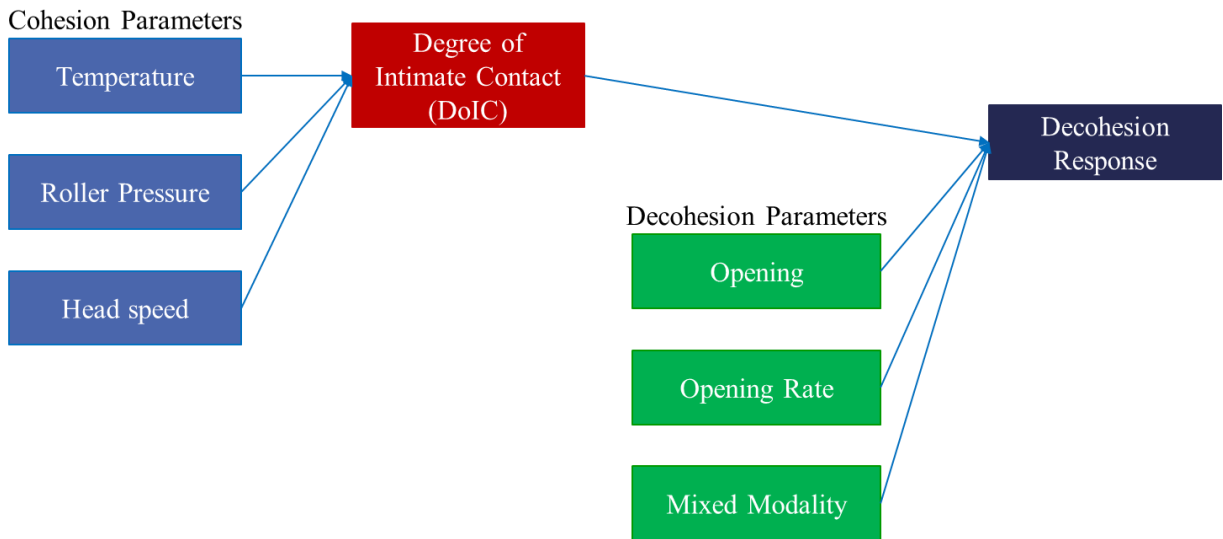


Figure 3 Schematic of dependency diagram.

## 2. EXPERIMENTAL

Characterization of prepreg tack was performed using the probe tack test technique. The advantage of this test is the ability to decouple parameters which drive cohesion and decohesion, with the only exception being the temperature and humidity conditions within a test. The material used in the study was IM7/8552-1 slit tape prepreg. Two methodologies and subsequent test parameters were investigated for the contact configuration between the probe and sample. A first design of experiments (DOE) was conducted using a displacement-controlled mode only where the normal force decreases as material flows out of the contact area [4]. A second DOE was conducted to include both a displacement and force-controlled mode within the same test. A comprehensive statistical analysis was previously reported by Wohl [4]; therefore, this paper focuses on the second DOE incorporating the displacement to force mode shift and application to the proposed tack model for AFP simulations. An image of the test set up for both design of experiments is shown below in Figure 4.

### 2.1 Methodology

Samples were prepared by placing 1-2 strips of slit tape on a sandblasted stainless steel rheometer lower flat plate with an applied pressure to ensure strong contact. Probe diameters of 4 and 8 mm were interrogated, and this required two strips of slit tape to be placed adjacent to one another for the 8 mm probe. The tape was placed across the lower flat plate and adhered using a custom design fixture which applied 66 psi uniformly over the surface of the prepreg. The custom fixture included a circular cavity in the middle to avoid contacting the location on the surface which the probe would interrogate. Further detail on the test approach can be found in Wohl [4].

Probe tack testing was performed on an Anton Paar USA Inc. MCR 520 TwinDrive™ Modular Rheometer equipped with an environmental controller (MHG 100 Humidity Generator). Samples were equilibrated at a defined temperature and humidity for one hour to ensure homogeneity prior to testing. The procedures for performing the probe tack test included:

1. Probe contact with the surface of interest at a defined crosshead speed until a defined contact force is achieved.
2. The probe held in contact for a given amount of time.
3. Retraction of the probe from the surface at a defined rate.

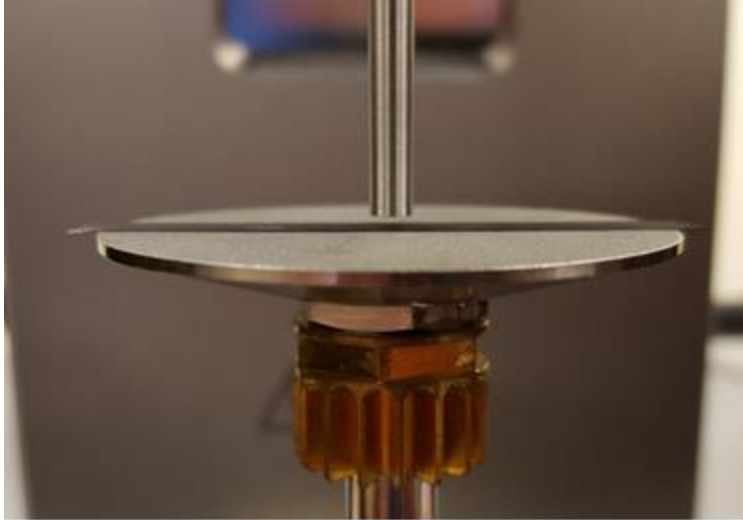


Figure 4. Image of the probe tack test in the ANTON Paar MCR 520 Courtesy of Chris Wohl (NASA Langley Research Center)

The test data output is shown in Figure 5, and the times when the mode switch occurs are identified. This configuration allows the probe to move, as shown by the displacement profile, to maintain a constant applied force on the sample throughout the contact dwell.

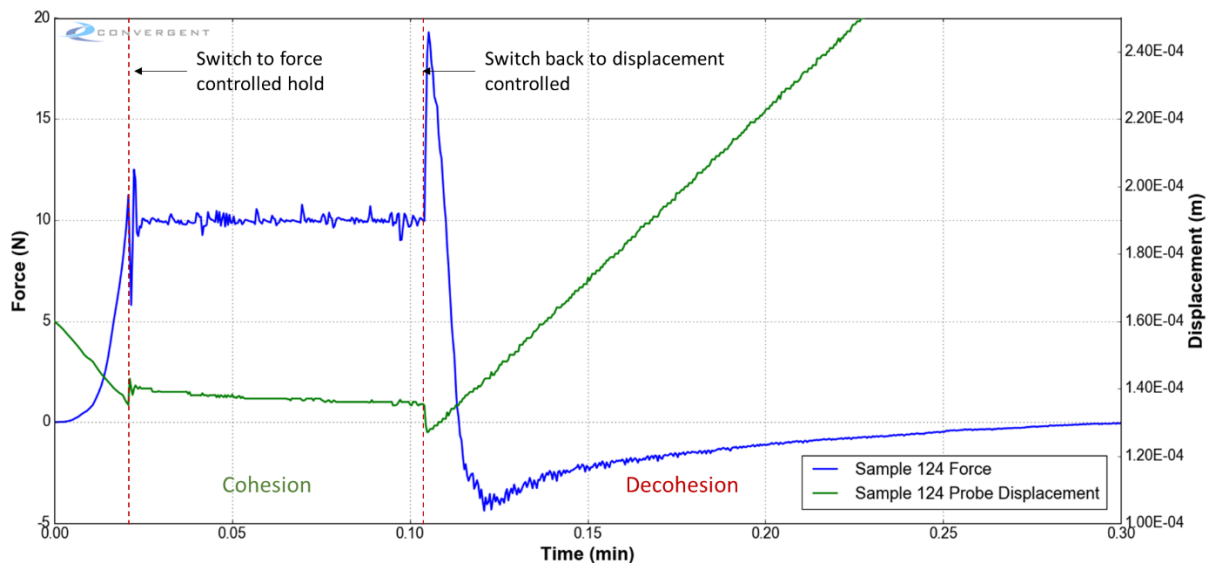


Figure 5. Image of probe tack test from DOE 2

DOE 2 test parameters were contact force, contact time, and temperature as shown below in Table 1. The focus of the DOE was to investigate the relationship between contact force and time on the potential variation observed during the decohesion stage. In this DOE, 55 samples were tested with a data capture rate of 2 points/sec.

Table 1. DOE 2 test parameters and ranges (55 samples)

Parameter	Units	Range	No. of Conditions
Contact force	N	1-30	9
Contact time	Sec	1-300	10
Temperature	°C	40-60	3
Humidity	%	40	1
Crosshead speed	mm/s	.0167	1
Probe diameter	mm	4	1

## 2.2 Experimental Results

The degree of cohesion between the probe and the prepreg was evaluated by investigating parameters such as the peak decohesion force, total Energy of Separation (EoS), as well as other characteristics of the decohesion regime (e.g. peak rate). EoS was calculated as the integral of tensile force per sample area with the displacement ( $\delta$ ), during the decohesion regime (Equation 1). The EoS and peak tack force or maximum tensile force during decohesion was evaluated for the varying test parameters.

$$\text{Energy of Separation (EoS)} = \int \frac{(\text{Force})}{(\text{Probe Area})} d\delta \quad (1)$$

Figure 6 shows a linear relationship between the decohesion peak force and the overall energy of separation for all tested samples. Additionally, there was a direct relationship between the peak force and the rate from the start of decohesion to the peak force, as shown in Figure 7. Specifically, a faster rate of opening corresponds to a higher peak decohesion force.

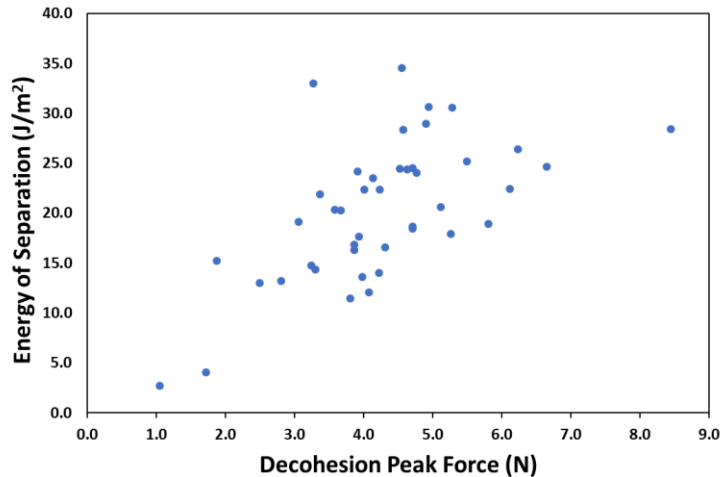


Figure 6 Energy of Separation as a function of decohesion peak force for all samples.

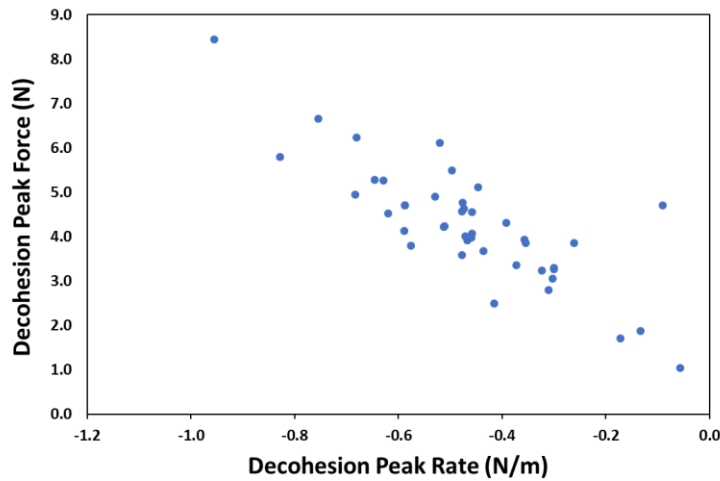


Figure 7 Decohesion peak force as a function of the decohesion peak rate for all test samples.

The decohesion peak force for varying contact force and contact time is summarized in Figure 8. The data show a general increase in the peak decohesion force with increasing contact force for varying contact times. Inspection of the data for an applied contact force of 10N showed a possible peak in the plateau region, e.g. a dwell time of 60 seconds results in a lower peak force than that of a dwell time of 30 seconds. This may be a true effect or test scatter; for a first generation tack model it will be assumed that the peak decohesion force plateaus past 15 seconds. The peak decohesion force also shows a general increase with respect to contact time up to 15 seconds where it begins to plateau, and the dwell time no longer affects the peak decohesion. At this point, it was assumed that the sample has achieved intimate contact with the probe surface after 15 seconds. It should be noted that typical AFP head speeds will be significantly quicker than the contact times in this study (0.5 to 2 seconds). Based on the data collected, this would indicate a lower degree of inter-diffusion between the two surfaces and therefore a lower degree of intimate contact. Understanding the upper bound of the degree of intimate contact was valuable in defining the scale for intimate contact.

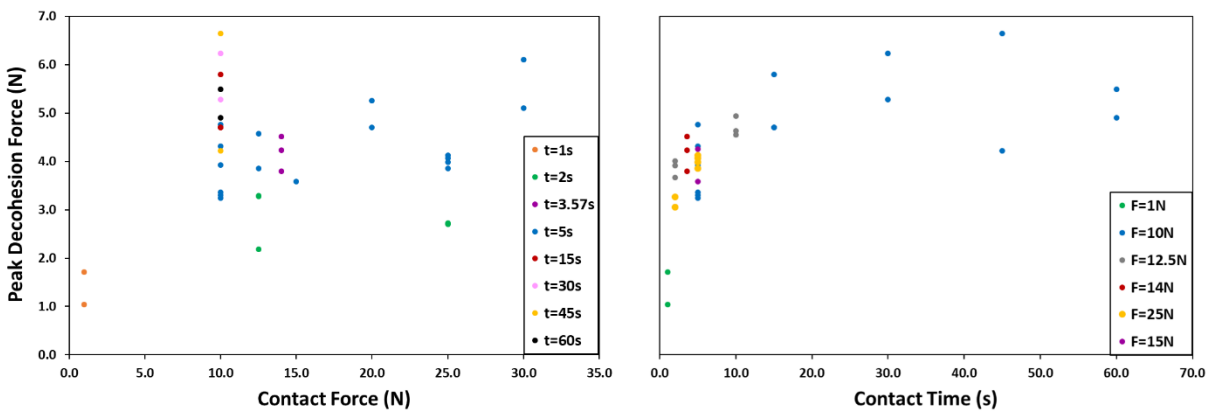


Figure 8 Peak Decohesion Force as a function of varying contact force and contact time for samples at 40°C and 40% humidity.

A closer examination of the raw test data for individual samples of varying dwell time and contact force is shown in Figure 9. For clarity, only a selected range of test parameters (including repeated tests) are included in the figure. As previously discussed, increasing dwell time and contact force resulted in a higher peak force and overall energy of separation. Additionally, a linear relationship between the EoS and the rate at which the force reaches the peak decohesion is shown in Figure 10. This included samples at 40°C and 40% relative humidity (RH) with highlighted samples corresponding to Figure 9.

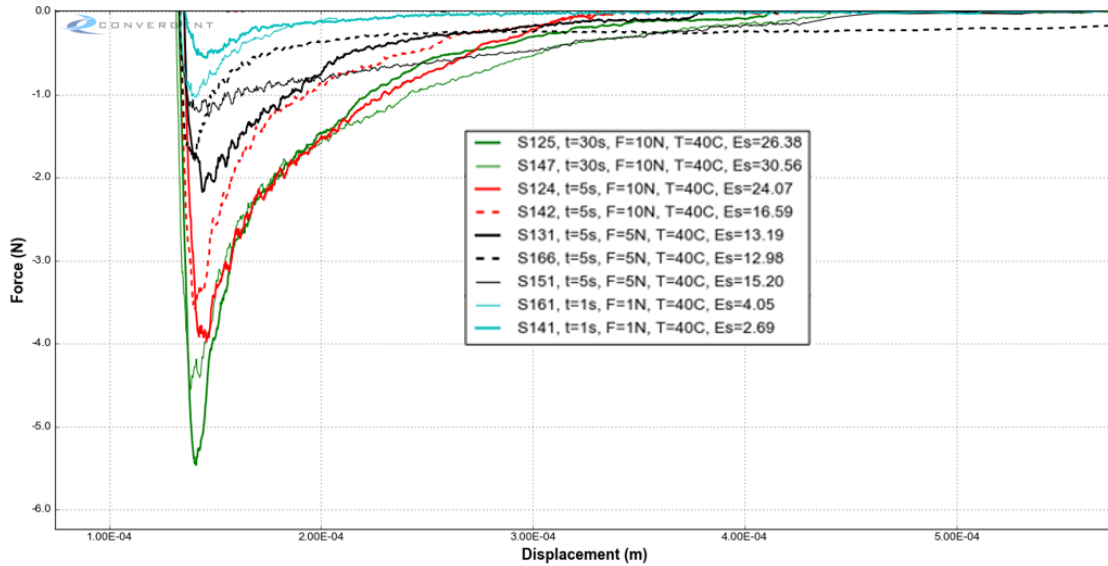


Figure 9 Test data from DOE 2 of the decohesion segment with varying contact time ( $t$ ) and applied contact force ( $F$ ) for a given temperature ( $T$ ) including the calculated Energy of Separation ( $E_s$ ) for an individual sample ( $S$ ).

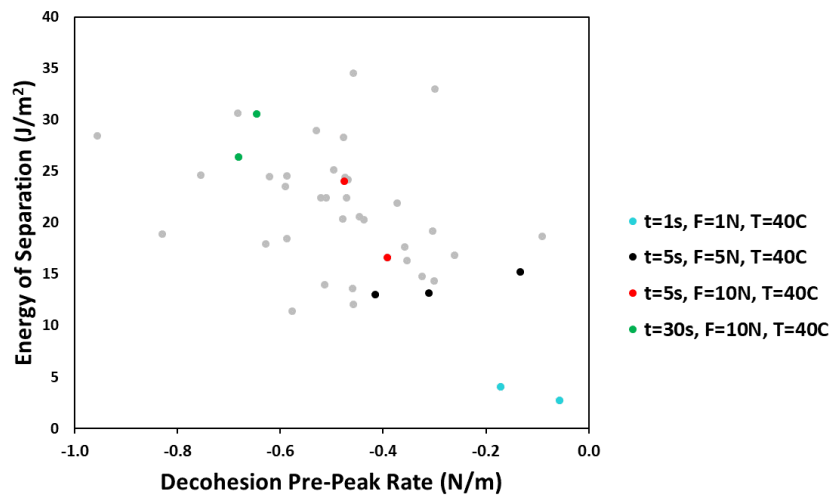


Figure 10 Energy of separation as a function of the rate at which the force reaches the decohesion peak for varying contact time ( $t$ ), applied contact force ( $F$ ), and temperature ( $T$ ) corresponding to the test data in Figure 9



### 3. TACK MODELING FRAMEWORK

Based on the trends observed in the experimental work above, a modeling framework was proposed based on the decohesion of the two surfaces. The phenomena interrogated in the DOE has been used to establish a structure for such a rate dependent model.

#### 3.1 Cohesion Stage

To achieve cohesion between two prepreg faces, the two sides have to be brought into physical contact (shown as nominal contact in Figure 11). When physical contact is established and resin on both sides come in contact, mixing and inner-diffusion lead to formation of cohesion between the two sides. Degree of Intimate Contact (DoIC) is an intermediate state variable introduced here to quantify the state of cohesion between two faces in contact. DoIC is a factor between 0, corresponding to no cohesion, and 1.0, corresponding to complete inter-diffusion and full cohesion with elimination of any gap or boundary between layers. Other physical phenomena such as surface tension and interlocking of fibers may also affect the evolution of DoIC.

Flow of resin into the micro gaps formed between the two surfaces is a key mechanism in achieving intimate contact. Degree of cure, surface roughness, and moisture content are other important parameters that affect the tack response through DoIC. It should be noted that DoIC is an intermediate state variable and would not be measured in-situ, but rather, characterized based on its contribution to decohesion behavior.

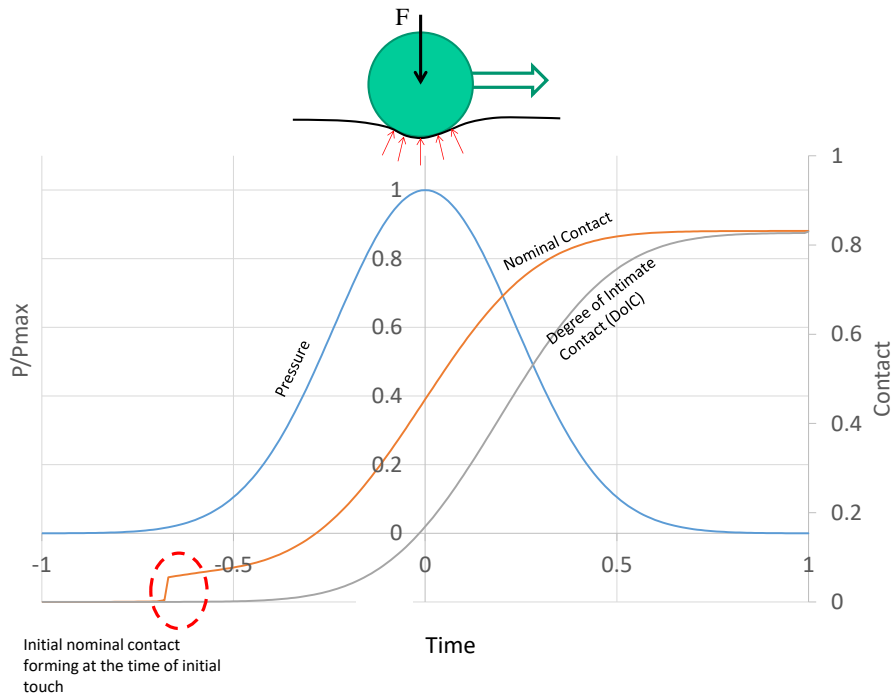


Figure 11. Development of Nominal Contact and Degree of Intimate Contact upon tow deposition and compaction by AFP head.

### 3.2 Rate-dependent Model for Decohesion

Peeling experiments performed by Crossley and co-workers show a strong dependency of tack response on peeling rate and temperature [2]. To capture the dependencies by the tack model, a rate-dependent model was proposed for the decohesion stage in generalized form as Equation 2:

$$\sigma = \sigma(\delta, \dot{\delta}, T, SDV, FLV) \quad (2)$$

where  $\sigma$  is the traction vector transferred between the two surfaces during decohesion.  $\delta$  and  $\dot{\delta}$  are the opening and opening rate vector that includes both normal and sliding components.  $T$  is the temperature,  $SDV$  and  $FLV$  are the vectors of state variables and field variables, respectively.

As discussed in Section 2, the decohesion response can be divided in two distinct regions: pre-peak and post-peak as shown in Figure 12 below:

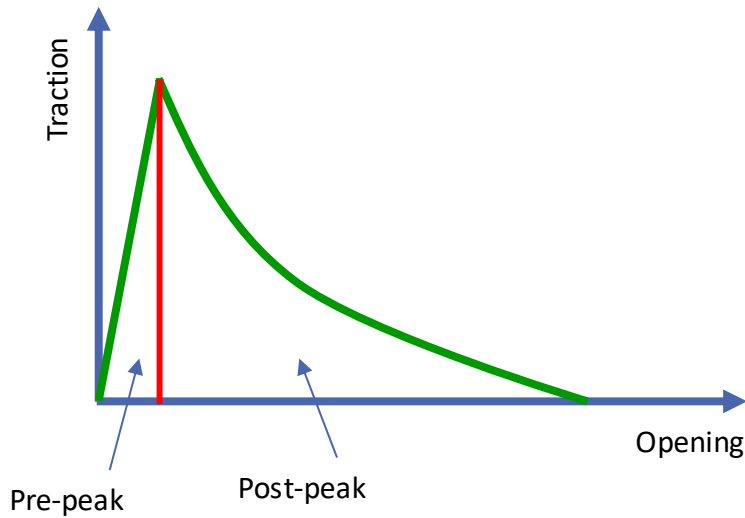


Figure 12 Schematic of the traction-opening in mode I.

To achieve temperature and rate dependencies observed in the experiments, a viscoelastic formulation was proposed to describe the pre-peak response as shown in Figure 13 below:

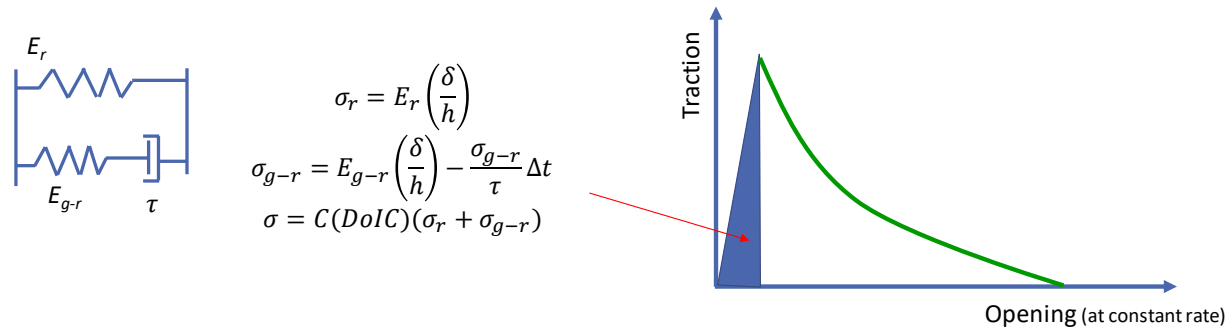


Figure 13 Viscoelastic description of the pre-peak tack response.

where  $E_r$  and  $E_g$  are the rubbery and glassy moduli of the resin,  $\delta$  is the opening,  $h$  is the thickness of the inter-ply interface and  $\tau$  is the time scale associated with stress relaxation. The parameter  $C(\text{DoIC})$  introduces the dependency on the degree of intimate contact to the pre-peak response. The concept of time-temperature superposition was employed to shift the relaxation time at different temperatures. For the shear mode,  $E_r$  and  $E_g$  were replaced by  $G_r$  and  $G_g$  which are the rubbery and glassy shear moduli of the resin.

A mixed-mode opening-based criteria was employed here to describe the peak condition as shown in Equation 3:

$$\left(\frac{\delta_n}{\delta_{ni}}\right)^2 + \left(\frac{\delta_{t2}}{\delta_{t2i}}\right)^2 + \left(\frac{\delta_{t3}}{\delta_{t3i}}\right)^2 = 1 \quad (3)$$

where  $\delta_n$ ,  $\delta_{t2}$  and  $\delta_{t3}$  represent the normal opening and two shear sliding components and  $\delta_{ni}$ ,  $\delta_{t2i}$ ,  $\delta_{t3i}$  are the critical opening and sliding displacements at the peak.

The post-peak tack response observed in probe tack tests show an exponential decay shape as shown in Figure 14. Therefore, an exponential decay function was chosen to describe the post-peak tack response, shown in Equation 4:

$$R = \exp\left(-\left(\left(\frac{\delta_n}{\delta_{nc}}\right)^2 + \left(\frac{\delta_{t2}}{\delta_{t2c}}\right)^2 + \left(\frac{\delta_{t3}}{\delta_{t3c}}\right)^2\right)^\gamma\right) \quad (4)$$

where  $R$  is mixed-mode reduction factor expressed in terms of opening and sliding. The post-peak traction is then expressed as  $\sigma_{\text{post-peak}} = R \sigma_{\text{Peak}}$ .

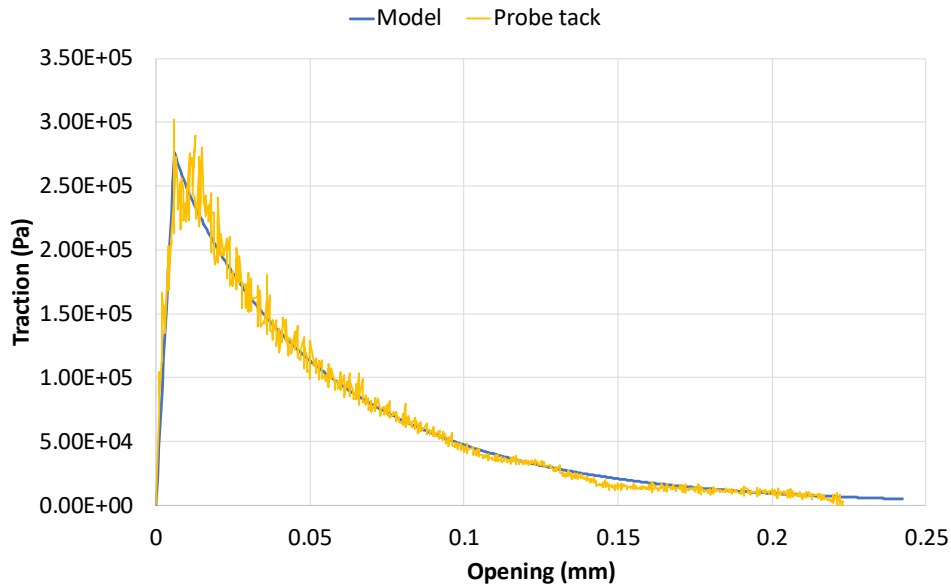


Figure 14. Tack model's pre-peak and post-peak exponential decay overlaid on probe tack measurement.

### 3.3 Tack Model Implementation

The probe tack model was implemented as a user-defined contact within COMPRO's Common Component Architecture (CCA). The user-defined contact model describes the interaction between the two surfaces in contact as shown in Figure 15. The model is responsible to define both normal and tangential traction components.

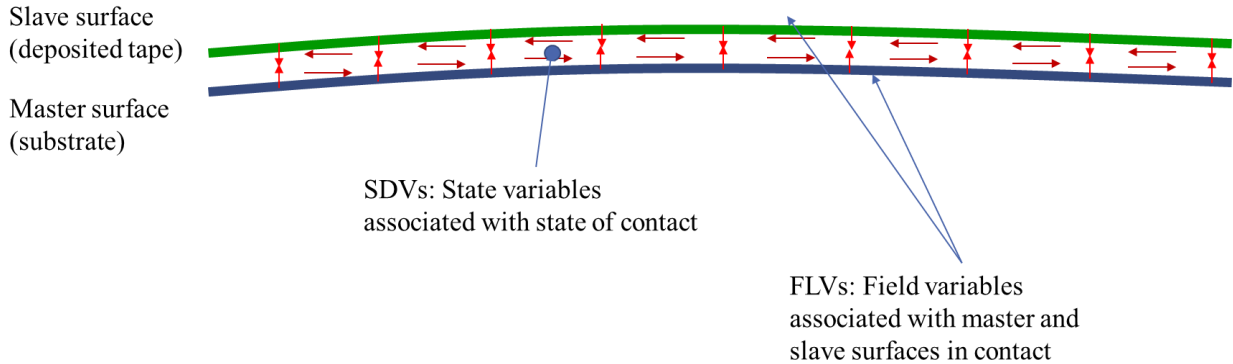


Figure 15. Schematic of the master and slave surfaces in contact.

Being part of COMPRO, the Tack model has access to the components in the CCA Library that describe evolution of resin properties during process (e.g. cure kinetics, viscosity, resin modulus to name a few). A schematic of the model implementation is shown below in Figure 16.

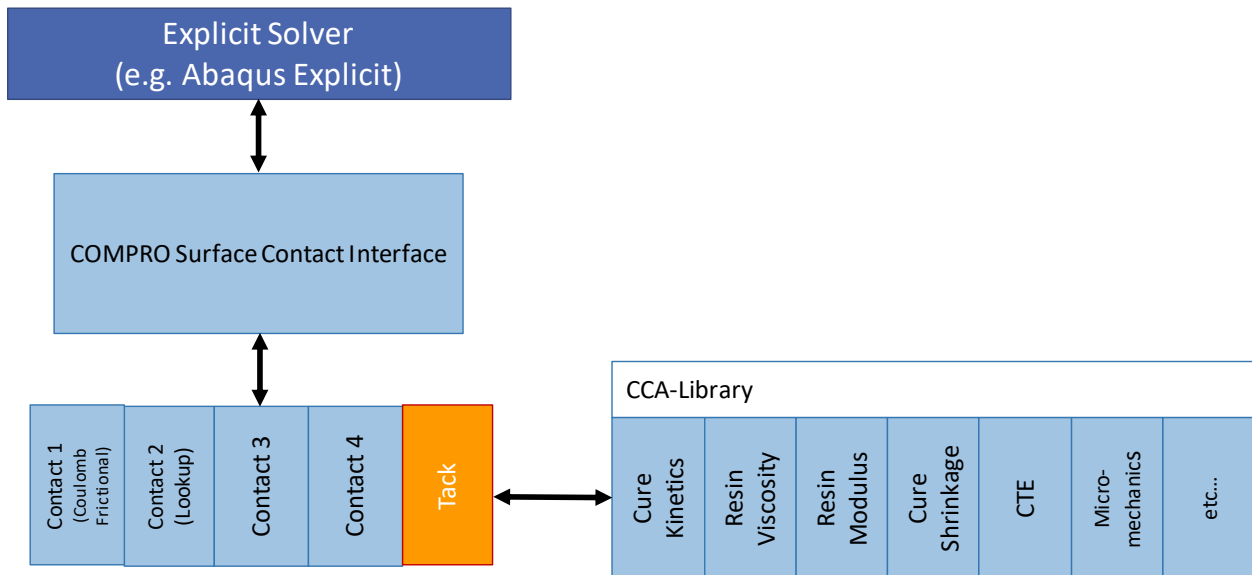


Figure 16. Implementation of the tack model within COMPRO framework.

## 4. CONTINUED EFFORTS

To reduce noise and increase the level of confidence and accuracy in the data analysis, smoothing and additional curve fitting techniques are currently being implemented for the probe tack data in

order to accurately calibrate the tack model. The trailing end of the decohesion force has a strong influence on the total energy of separation. A study determining the effect of this on the EoS calculation will be investigated. Characterization to this point has focused on contact between prepreg slit tape and a stainless steel probe to capture the dependencies of decohesion on input parameters such as temperature, contact force and contact time. Further techniques to gather information regarding the material properties and contact state are being investigated. Future work will expand to include prepreg to prepreg interactions and mixed mode separation in the form of peel tests.

## 5. SUMMARY

Probe tack characterization was performed to evaluate the tack response of Hexcel IM7/8552-1 prepreg for the purpose of modeling AFP defects. A DOE has been performed to interrogate the parameter space of interest. Strong correlations were found between the peak tack force and the energy of separation and the decohesion peak rate and energy of separation. A plateau in the peak decohesion force was observed beyond a contact time of 15 seconds indicating that intimate contact between the two surfaces was achieved. Based on these observations, a rate dependent tack model is proposed which focuses on the decohesion peak rate, peak tack force and a decay factor. A tack model was proposed based on the probe tack experimental methods and analysis. In order to estimate cohesion, specifically the Degree of intimate Contact (DoIC), a rate-dependent decohesion tack model describing a mixed-mode opening and an exponential decay for the post-peak decohesion response was developed. The model framework will be implemented within COMPRO's Common Component Architecture (CCA) which includes various resin properties. The developed tack model is being incorporated in the physics-based AFP modeling frame work, shown in Figure 1. The preliminary simulations show that the model is capable of predicting the defect formation trends observed in AFP trials.

## 6. REFERENCES

1. Ahn, K.J. et al., 1992. Analysis and characterization of prepreg tack. *Polymer Composites*, 13(3), pp.197–206.
2. Crossley, R.J., Schubel, P.J. & De Focatiis, D.S.A., 2013. Time-temperature equivalence in the tack and dynamic stiffness of polymer prepreg and its application to automated composites manufacturing. *Composites Part A: Applied Science and Manufacturing*, 52, pp.126–133. Available at: <http://dx.doi.org/10.1016/j.compositesa.2013.05.002>.
3. Dubois, O., Le Cam, J.-B. & Béakou, A., 2010. Experimental Analysis of Prepreg Tack. *Experimental Mechanics*, 50(5), pp.599–606.
4. Wohl, C.; Palmieri, F.; Forghani, A.; Hickmott, C.; Bedayat, H.; Coxon, B.; Poursartip, A.; Grimsley, B. "Tack Measurements of Prepreg Tape at Variable Temperature and Humidity." *CAMX Technical Conference*. Orlando, FL United States of America, Dec 12-14, 2017. The Composites and Advanced Materials Expo.

5. Zhou, X. et al., 2015. Recent Advances in Synthesis of Waterborne Polyurethane and Their Application in Water-based Ink: A Review. *Journal of Materials Science & Technology*, 31(7), pp.708–722.
6. Forghani, A.; Hickmott, C.; Housman, B.; Wohl, C.; Grimsley, B.; Coxon, B.; Poursartip, A. "A Physics-Based Modelling Framework for Simulation of Prepreg Tack in AFP Process." *SAMPE Technical Conference*. Seattle, WA United States of America, May 22-25, 2017. Society for the Advancement of Material and Process Engineering.